Trace cancer biomarker quantification using polystyrene-functionalized gold nanorods

Jian Wu, Wei Li, Ghazal Hajisalem, Ariella Lukach, Eugenia Kumacheva, Fraser Hof, and Reuven Gordon

November 2014

This article was originally published at:

http://dx.doi.org/10.1364/BOE.5.004101

Biomedical Optics EXPRESS

Trace cancer biomarker quantification using polystyrene-functionalized gold nanorods

Jian Wu,[1] Wei Li,[2] Ghazal Hajisalem,[1] Ariella Lukach,[3] Eugenia Kumacheva,[3] Fraser Hof,[2] and Reuven Gordon[1,*]

[1]*Department of Electrical Engineering, University of Victoria, Victoria, British Columbia V8W 2Y2, Canada*
[2]*Department of Chemistry, University of Victoria, Victoria, British Columbia V8W 3V6, Canada*
[3] *Department of Chemistry, University of Toronto, 80 Saint George Street, Toronto, Ontario M5S 3H6, Canada*
[*]*rgordon@uvic.ca*

Abstract: We demonstrate the application of polystyrene-functionalized gold nanorods (AuNRs) as a platform for surface enhanced Raman scattering (SERS) quantification of the exogenous cancer biomarker Acetyl Amantadine (AcAm). We utilize the hydrophobicity of the polystyrene attached to the AuNR surface to capture the hydrophobic AcAm from solution, followed by drying and detection using SERS. We achieve a detection limit of 16 ng/mL using this platform. This result shows clinical potential for low-cost early cancer detection.

OCIS codes: (240.6695) Surface-enhanced Raman scattering; (240.6680) Surface plasmons; (280.4788) Optical sensing and sensors.

References and links

1. T. Thomas and T. J. Thomas, "Polyamine metabolism and cancer," J. Cell. Mol. Med. **7**(2), 113–126 (2003).
2. A. P. Bras, J. Jänne, C. W. Porter, and D. S. Sitar, "Spermidine/Spermine N 1-Acetyltransferase Catalyzes Amantadine Acetylation," Drug Metab. Dispos. **29**(5), 676–680 (2001).
3. A. P. Bras, H. R. Hoff, F. Y. Aoki, and D. S. Sitar, "Amantadine acetylation may be effected by acetyltransferases other than NAT1 or NAT2," Can. J. Physiol. Pharmacol. **76**(7-8), 701–706 (1998).
4. D. S. Sitar, A. P. Bras, A. Maksymiuk, A. Pabbies, L. Brande, and B. W. Blakely, "Amantadine acetylation as a biomarker for malignancy," Clin. Pharmacol. Ther. **79**(2), 10 (2006).
5. D. S. Sitar and A. P. M. Bras, "Method for Assaying Non-Spermine/Spermidine Activity of N1-Acetyltransferase (SSAT)," U.S. Patent, US6811967 B2, 2004.
6. N. B. Colthup, L. H. Daly, and S. E. Wiberley, *Introduction to infrared and Raman spectroscopy* (Elsevier, 1990).
7. S. Wachsmann-Hogiu, T. Weeks, and T. Huser, "Chemical analysis in vivo and in vitro by Raman spectroscopy - from single cells to humans," Curr. Opin. Biotechnol. **20**(1), 63–73 (2009).
8. T. Vo-Dinh, L. R. Allain, and D. L. Stokes, "Cancer gene detection using surface-enhanced Raman scattering (SERS)," J. Raman Spectrosc. **33**(7), 511–516 (2002).
9. K. Kneipp, H. Kneipp, I. Itzkan, R. R. Dasari, and M. S. Feld, "Ultrasensitive chemical analysis by Raman spectroscopy," Chem. Rev. **99**(10), 2957–2976 (1999).
10. R. L. McCreery, *Raman spectroscopy for chemical analysis* (John Wiley & Sons, 2005).
11. K. Kneipp and H. Kneipp, "Single molecule Raman scattering," Appl. Spectrosc. **60**(12), 322–334 (2006).
12. S. Nie and S. R. Emory, "Probing single molecules and single nanoparticles by surface-enhanced Raman scattering," Science **275**(5303), 1102–1106 (1997).
13. K. Kneipp, Y. Wang, H. Kneipp, L. T. Perelman, I. Itzkan, R. R. Dasari, and M. S. Feld, "Single molecule detection using surface-enhanced Raman scattering (SERS)," Phys. Rev. Lett. **78**(9), 1667–1670 (1997).
14. H. Xu, E. J. Bjerneld, M. Käll, and L. Börjesson, "Spectroscopy of single hemoglobin molecules by surface enhanced Raman scattering," Phys. Rev. Lett. **83**(21), 4357–4360 (1999).
15. W. W. Yu and I. M. White, "Inkjet-printed paper-based SERS dipsticks and swabs for trace chemical detection," Analyst (Lond.) **138**(4), 1020–1025 (2013).
16. W. W. Yu and I. M. White, "Chromatographic separation and detection of target analytes from complex samples using inkjet printed SERS substrates," Analyst (Lond.) **138**(13), 3679–3686 (2013).
17. B. Nikoobakht and M. A. El-Sayed, "Surface-enhanced Raman scattering studies on aggregated gold nanorods," J. Phys. Chem. A **107**(18), 3372–3378 (2003).
18. S. L. Smitha, K. G. Gopchandran, T. R. Ravindran, and V. S. Prasad, "Gold nanorods with finely tunable longitudinal surface plasmon resonance as SERS substrates," Nanotechnology **22**(26), 265705 (2011).
19. B. Nikoobakht, J. Wang, and M. A. El-Sayed, "Surface-enhanced Raman scattering of molecules adsorbed on gold nanorods: off-surface plasmon resonance condition," Chem. Phys. Lett. **366**(1-2), 17–23 (2002).

#224379 - $15.00 USD Received 7 Oct 2014; revised 27 Oct 2014; accepted 27 Oct 2014; published 3 Nov 2014

20. A. Lee, G. F. S. Andrade, A. Ahmed, M. L. Souza, N. Coombs, E. Tumarkin, K. Liu, R. Gordon, A. G. Brolo, and E. Kumacheva, "Probing Dynamic Generation of Hot-Spots in Self-Assembled Chains of Gold Nanorods by Surface-Enhanced Raman Scattering," J. Am. Chem. Soc. **133**(19), 7563–7570 (2011).
21. A. Lee, A. Ahmed, D. P. dos Santos, N. Coombs, J. I. Park, R. Gordon, A. G. Brolo, and E. Kumacheva, "Side-by-side assembly of gold nanorods reduces ensemble-averaged SERS intensity," J. Phys. Chem. C **116**(9), 5538–5545 (2012).
22. Z. Huang, G. Meng, Q. Huang, B. Chen, C. Zhu, and Z. Zhang, "Large-area Ag nanorod array substrates for SERS: AAO template-assisted fabrication, functionalization, and application in detection PCBs," J. Raman Spectrosc. **44**(2), 240–246 (2013).
23. S. T. Jones, R. W. Taylor, R. Esteban, E. K. Abo-Hamed, P. H. Bomans, N. A. Sommerdijk, and O. A. Scherman, "Gold Nanorods with Sub-Nanometer Separation using Cucurbit[n]uril for SERS Applications," Small doi 10.1002/smll.201401063 (posted 28 July 2014, in press).
24. H. Takayama, S. Takahashi, T. Moriya, H. Osada, Y. Iwabuchi, and N. Kanoh, "Detection of Cytochrome P450 Substrates by Using a Small-Molecule Droplet Array on an NADH-Immobilized Solid Surface," ChemBioChem **12**(18), 2748–2752 (2011).
25. B. Nikoobakht and M. A. El-Sayed, "Preparation and growth mechanism of gold nanorods (NRs) using seed-mediated growth method," Chem. Mater. **15**(10), 1957–1962 (2003).
26. A. Lukach, K. Liu, H. Therien-Aubin, and E. Kumacheva, "Controlling the Degree of Polymerization, Bond Lengths, and Bond Angles of Plasmonic Polymers," J. Am. Chem. Soc. **134**(45), 18853–18859 (2012).
27. G. Hajisalem, Q. Min, R. Gelfand, and R. Gordon, "Effect of surface roughness on self-assembled monolayer plasmonic ruler in nonlocal regime," Opt. Express **22**(8), 9604–9610 (2014).
28. C. Noguez, "Surface plasmons on metal nanoparticles: the influence of shape and physical environment," J. Phys. Chem. C **111**(10), 3806–3819 (2007).
29. A. F. Palonpon, J. Ando, H. Yamakoshi, K. Dodo, M. Sodeoka, S. Kawata, and K. Fujita, "Raman and SERS microscopy for molecular imaging of live cells," Nat. Protoc. **8**(4), 677–692 (2013).
30. R. Y. Sato-Berrú and J. M. Saniger, "Application of principal component analysis to discriminate the Raman spectra of functionalized multiwalled carbon nanotubes," J. Raman Spectrosc. **37**(11), 1302–1306 (2006).
31. L. Zhang, Q. Li, W. Tao, B. Yu, and Y. Du, "Quantitative analysis of thymine with surface-enhanced Raman spectroscopy and partial least squares (PLS) regression," Anal. Bioanal. Chem. **398**(4), 1827–1832 (2010).
32. D. S. Sitar, A. P. Bras, A. Maksymiuk, K. M. Cheng, and H. Zhou, "Progress in the development of SSAT1 activity as a biomarker for diagnosis of cancer," presented at the BIT Life Sciences' Annual World Cancer Congress, Beijing, 22–25 Jun. 2009.
33. R. W. Taylor, T. C. Lee, O. A. Scherman, R. Esteban, J. Aizpurua, F. M. Huang, J. J. Baumberg, and S. Mahajan, "Precise subnanometer plasmonic junctions for SERS within gold nanoparticle assemblies using cucurbit[n]uril "glue"," ACS Nano **5**(5), 3878–3887 (2011).
34. S. Mahajan, T. C. Lee, F. Biedermann, J. T. Hugall, J. J. Baumberg, and O. A. Scherman, "Raman and SERS spectroscopy of cucurbit[n]urils," Phys. Chem. Chem. Phys. **12**(35), 10429–10433 (2010).
35. R. W. Taylor, R. J. Coulston, F. Biedermann, S. Mahajan, J. J. Baumberg, and O. A. Scherman, "In Situ SERS Monitoring of Photochemistry within a Nanojunction Reactor," Nano Lett. **13**(12), 5985–5990 (2013).
36. G. Cao, G. Hajisalem, W. Li, F. Hof, and R. Gordon, "Quantification of an exogenous cancer biomarker in urinalysis by Raman Spectroscopy," Analyst (Lond.) **139**(21), 5375–5378 (2014).

1. Introduction

Acetyl Amantadine (AcAm) is the acetylated product of Amantadine (Am) created by the action of the enzyme Spermidine/Spermine N1 Acetyltransferase (SSAT) in human bodies. SSAT's activity is significantly up-regulated in a wide variety of tumor types, making AcAm a candidate exogenous biomarker for cancer screening [1–4]. Current methods for quantification of AcAm in urine use liquid chromatography with tandem mass spectrometery (LCMS) [5]. The disadvantages of LCMS include high per-sample cost, long analytical time, and high instrument cost, thereby hindering its widescale usage. A lower cost and faster approach to quantification with sensitivity at clinically required levels is highly desirable.

Raman spectroscopy provides specific "fingerprint" information for molecules [6]. It is a promising optical technique for cancer diagnosis [7, 8] and chemical detection [9, 10]. Suffering from the low signal caused by a small scattering cross section (typically 10^{-30} to 10^{-25} cm^{-2} per molecule [11]), conventional Raman spectroscopy presents great challenges for clinical adoption. Surface enhanced Raman scattering (SERS) enhances the Raman signal by exciting the localized surface plasmon resonance (LSPR) on plasmonic materials (e.g., gold, silver, and copper) of nanoscale dimensions [12–14]. Thus it can be used to improve greatly the sensitivity in quantitative analysis [15, 16].

Gold nanorods (AuNRs) are suitable as SERS substrates [17, 18]. By tuning the aspect ratio of AuNRs through minor modifications of the synthetic procedure, LSPR can be tuned to enhance coupling in the excitation/collection wavelength range [19]. The AuNR ends

#224379 - $15.00 USD Received 7 Oct 2014; revised 27 Oct 2014; accepted 27 Oct 2014; published 3 Nov 2014

produce the highest electric field intensity [20, 21], therefore analytes situated at the AuNR ends will experience the greatest Raman enhancement. A previous report used thiolated β-cyclodextrin (β-CD) as a binding pocket to capture analytes to the NR surface [22]. Another report utilized cucurbit[n]urils (CB[n]s) as the binding pockets and rigid spacers to align AuNRs end-to-end and precisely control the AuNR separation [23].

In this paper, we investigate the use of AuNRs as a SERS substrate to quantify the amount of AcAm in solution. We functionalize the AuNR surface with polystyrene, and use the hydrophobicity of the polystyrene as a more general binding agent that effectively collects AcAm from solution. We present quantitative analysis of the Raman spectra and the detection limit of the platform.

2. Experiments

2.1 AcAm synthesis

AcAm was synthesized following a previously developed protocol [24]. 2 g Amantadine (Tokyo Chemical Industry) was dissolved in 30 mL dichloromethane under nitrogen atmosphere. 3.77 g triethylamine was then added to the Am solution and stirred for 5 min. 2.17 g acetic anhydride was added to the mixture solution and stirred for 1 h. Water was added, and the aqueous layer was extracted using a separatory funnel. The combined organic extracts were dried over sodium sulfate, and then filtered. The mixture was concentrated to dryness on a rotary evaporator. High vacuum was applied to obtain AcAm as white solid form determined to be greater than 98% pure by 1H NMR analysis.

2.2 Gold nanorods synthesis

AuNRs were synthesized by the seed-mediated growth method [25]. Briefly, seed nanoparticles were synthesized by mixing $HAuCl_4$ solution (0.12 mL, 15 mM) with an aqueous solution of hexadecyltrimethylammoniumbromide (CTAB) (2.5 g, 0.20 M), 1 mL of deionized water, and 0.60 mL of ice-cold 0.010 M $NaBH_4$. The growth solution was prepared by mixing CTAB solution (5.36 g, 0.20 M), 4 mL deionized water, $AgNO_3$ (0.4 mL, 4 mM), $HAuCl_4$ (0.5 mL, 15 mM), ascorbic acid (0.124 mL, 0.0788 M), and 0.1 mL of the 45-min aged seed solution. The growth solution turned from colorless to reddish brown following incubation overnight at 27 °C. The concentrated AuNRs were then sonicated with 0.2 mg thiol-terminated polystyrene (Polymer Source Inc.) in 1 g tetrahydrofuran (THF) for 30 min to initiate the exchange of CTAB ligands at the NR ends with polystyrene. After incubation overnight at room temperature, the AuNRs were purified by eight centrifugation cycles at 9000 rpm for 30 min to remove excess polystyrene. The AuNRs were characterized by electron microscopy and extinction measurements [26]. The concentrated polystyrene-functionalized AuNRs were then redispersed in THF to form a stock solution.

2.3 Sample preparation

AuNRs were first dried from the stock solution and then redissolved in acetone (absorbance 0.92 at 760 nm). AcAm was dissolved in acetone at varying concentrations from 400 ng/mL to 10 μg/mL. 10 μL AcAm solution was added to 240 μL deionized water in a glass insert (300 μL size, Sigma Aldrich) with resultant concentrations from 16 ng/mL to 400 ng/mL. 50 μL NR solution was then added to the diluted AcAm solution. The mixture solution was sonicated for 5 min for thorough mixing. The solution was then incubated for 6 h at room temperature for the AcAm adsorption. After 20 min centrifugation at 6000 rpm, the subnatant was drop-coated onto a commercial Au-coated slide (EMF Corp.) for further characterization and Raman measurement.

#224379 - $15.00 USD Received 7 Oct 2014; revised 27 Oct 2014; accepted 27 Oct 2014; published 3 Nov 2014

2.4 Instrumentation

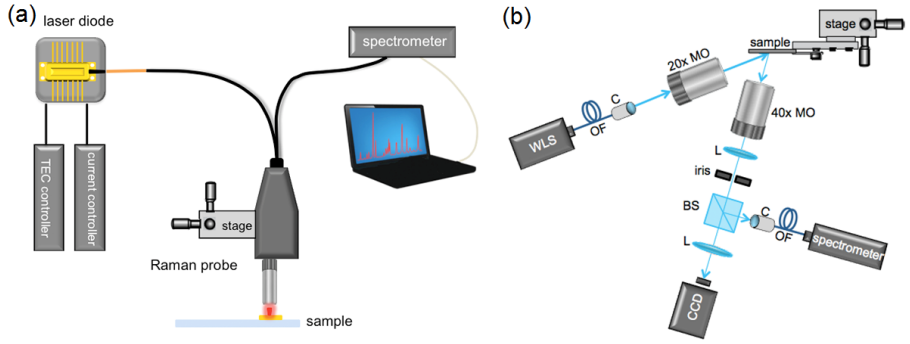

Fig. 1. (a) The Raman measurement setup. (b) The DF scattering measurement setup. WLS = white light source, OF = optical fiber, C = collimator, MO = microscope objective lens, L = lens, BS = beam splitter.

Figure 1(a) shows the Raman measurement setup. A 785 nm fiber-coupled laser diode (Innovative Photonic Solution, 30 mW) was used for excitation. A portable Raman probe (InPhotonics) was used for excitation, collection, and filtering. A spectrometer (QE65 pro, Ocean Optics Inc.) was used for detection. The Raman probe was mounted on a 3-axis linear translation stage for fine adjustment. 16 spectra were acquired for each sample at different random locations with 30 s integration time and 5 scans-to-average for each spectrum.

Figure 1(b) shows the dark-field (DF) scattering measurement setup. A collimated white light source (LS-1-LL, Ocean Optics Inc.) was focused onto the sample by a 20 × microscope objective (0.42 NA, Mitutoyo Plan Apo) at 70° to the surface normal. The off-normal configuration has been used to excite the LSPR of the nanoparticle-metal film [27]. The scattered light from the sample was collected at 15° to the surface normal by a 40 × microscope objective (0.68 NA, Zeiss). The scattered beam was split into two beams by a 50-50 beam splitter. One beam was directed into a CCD camera (GC660, Allied Vision Technologies) to take the DF scattering image. The other beam was directed into a spectrometer (QE65000, Ocean Optics Inc.) to take the DF scattering spectrum.

A scanning electron microscopy (SEM) image of the sample was obtained using a Hitachi S-4800 field emission SEM. UV-visible absorbance measurements of the AuNR solution were acquired using a SpectraMax M5 multi-mode microplate reader.

3. Results and discussion

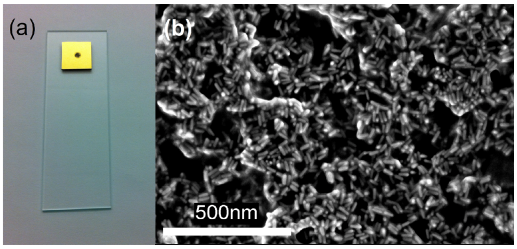

Fig. 2. (a) The prepared sample picture. The dried AuNR sample is located at the center of the Au-coated slide. The diameter of the spot is about 5 mm. (b) The SEM image of the dried AuNR sample. SEM imaging was carried out at 2 kV.

Figure 2(a) shows a picture of the prepared sample for detection. The dried AuNR sample is located at the center of the Au-coated slide. The diameter of the spot is about 5 mm. Figure 2(b) shows an SEM image of the dried AuNR sample. SEM imaging was carried out at 2 kV, which is suitable for imaging Au materials. The SEM image shows the AuNRs are aggregated

#224379 - $15.00 USD Received 7 Oct 2014; revised 27 Oct 2014; accepted 27 Oct 2014; published 3 Nov 2014

with random orientation in the dried spot. Nominally, the AuNRs have a length of 38 nm and a diameter of 10 nm. The aspect ratio is therefore 3.8.

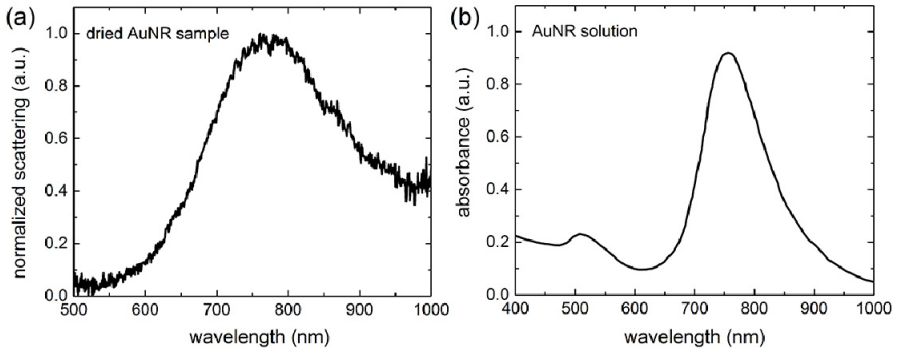

Fig. 3. (a) Normalized DF scattering spectrum of the dried AuNR sample. The LSPR peak is located at 775 nm (b) UV-visible absorbance spectrum of the AuNR solution. The longitudinal LSPR peak is located at 760 nm.

Figure 3(a) shows the normalized DF scattering spectrum of the dried AuNR sample. The spectrum shows a LSPR peak around 775 nm. The Raman excitation wavelength 785 nm is close to the LSPR wavelength, thereby enhancing coupling and the Raman signal. Figure 3(b) shows the UV-visible absorbance spectrum of the AuNR solution for comparison. The longitudinal LSPR peak is located at 760 nm. There is a 15-nm red shift of the LSPR peak of the dried AuNR sample compared to the dispersed AuNR solution. The shift may come from the coupling between the AuNRs in the aggregate and the presence of the Au-coated slide [28]. The aspect ratio of individual AuNRs is the key parameter in achieving high SERS response from the aggregated AuNRs. Our SERS study on the CTAB Raman modes of the aggregated CTAB-coated AuNRs confirmed that the CTAB Raman signal could be enhanced by tuning the aspect ratio of individual AuNRs to the value used in the present work.

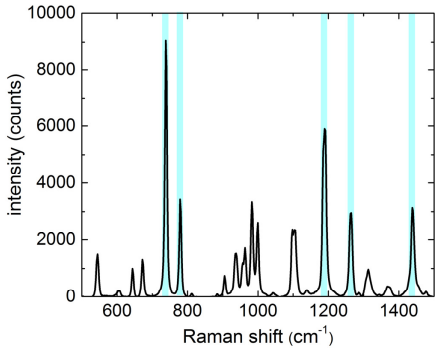

Fig. 4. Raman spectrum of AcAm powder. The characteristic peaks highlighted in cyan.

Figure 4 shows a representative Raman spectrum of AcAm powder. The characteristic peaks of AcAm (738 cm^{-1}, 779 cm^{-1}, 1189 cm^{-1}, 1265 cm^{-1}, and 1438 cm^{-1}) are highlighted in cyan.

Figure 5(a) shows the averaged Raman spectra of the sample prepared with 400 ng/mL AcAm, the blank sample without AcAm, and their difference spectrum (400 ng/mL AcAm – blank). Baselines of the Raman spectra were corrected by a spline interpolation method. The characteristic peaks (e.g., 1002 cm^{-1}) in the blank spectrum belong to the polystyrene. The ripple-like features (e.g., 700 cm^{-1} to 900 cm^{-1}) come from the etaloning effect of the CCD detector in the spectrometer and are spurious features [29]. The difference spectrum shows a good match to the spectrum of the AcAm powder, which reduces the etaloning and the background signal from the polystyrene.

#224379 - $15.00 USD Received 7 Oct 2014; revised 27 Oct 2014; accepted 27 Oct 2014; published 3 Nov 2014

Figure 5(b) shows a linear relation of the Raman intensity versus the AcAm concentration. The Raman intensity was calculated by summing the intensity values of the five characteristic peaks. The error bar of each data point stands for the standard error of the mean. Since each spectrum is averaged by 5 scans, it should have its own uncertainty. However, we did not implement the propagation of uncertainty in the final error calculation and relied solely on statistical analysis over multiple spectra. There are clear advantages of using more than one peak in quantification: more photon signal is acquired by multiple Raman peaks and the signal is spectrally distributed (i.e., less susceptible to local spectral artifacts – such as the polystyrene in this case). This supervised quantification method is effective for our application because the AcAm is the only analyte in our case. More sophisticated and unsupervised methods such as principal component analysis (PCA) and partial least squares (PLS) can be applied to multi-analyte situations [30, 31], but we do not attempt those here. The noise level highlighted in cyan is the intensity of the blank sample. The intensity level of the detection limit (16 ng/mL) equals the noise level plus three times of the standard error of the blank sample, which is close to the clinical threshold value (10 ng/mL) for a positive test in urine of North American subjects [32]. We use the standard error as opposed to the standard deviation in deducing the detection limit because each time we measure 16 spectra and use the mean value of the intensity to determine the AcAm concentration, rather than just measuring one single spectrum. Our analysis has confirmed that the data samples are well-fit to Gaussian distributions (not presented). Therefore, it is more appropriate to use the standard error of the mean to estimate the degree that the sample mean differs from the population mean than to use the standard deviation, which is used to estimate the degree that an individual value within the sample differs from the sample's mean. It should be noted that the detection limit could be improved by increasing the number of spectra obtained from one sample (equivalent to increasing the integration time), since the noise goes down as the square root of the number of spectra. But there is a trade-off between the detection limit and the acquisition time. For example, in principle the detection limit of 10 ng/mL could be achieved by increasing the number of spectra to 41, but this would almost triple the acquisition time. We chose 16 as the number of spectra to combine the promising detection limit and the reasonable acquisition time. In the future, we plan to improve the sensitivity and specificity by optimizing the capture agents (for example, using CBs [23, 33–35]) for higher AcAm affinity in real urine samples.

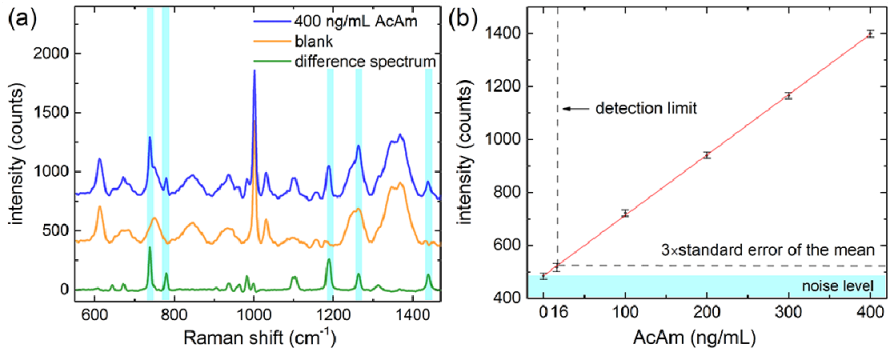

Fig. 5. (a) Averaged Raman spectra of the sample prepared with 400 ng/mL AcAm, the blank sample without AcAm, and their difference spectrum (400 ng/mL AcAm – blank). (b) Raman intensity (summed over the 5 selected AcAm peaks) as a function of the AcAm concentration. The noise level highlighted in cyan is the intensity of the blank sample. The detection limit of 16 ng/mL is indicated by the dashed line. The intensity level of the detection limit equals the noise level plus three times of the standard error of the blank sample. The error bar of each data point stands for the standard error of the mean.

This quantification approach presents rapid, reproducible and low-cost features that are desired for clinical adoption, as the acquisition of a single Raman spectrum is completed in 5 minutes. The results show good reproducibility when repeating over a period of 2 weeks.

#224379 - $15.00 USD Received 7 Oct 2014; revised 27 Oct 2014; accepted 27 Oct 2014; published 3 Nov 2014

Compared to our previous work using commercial Klarite substrates [36], the AuNR substrates are free of complex and expensive micro-fabrication processes, which can significantly reduce the cost. The economical Raman probe can be easily integrated into a compact and portable testing kit, showing a great potential for clinical and in field applications.

4. Conclusion

We presented a method for quantifying an exogenous cancer biomarker AcAm using polystyrene functionalized AuNRs as a SERS substrate, and multi-peak analysis for quantification. We achieved a detection limit of 16 ng/mL, which is promising for future clinical adoption. Future work can be focused on optimizing the capture agents such as CBs [23, 33–35] for higher AcAm affinity in real urine samples.

Acknowledgments

This work is funded by a Genome BC Proof-of-Concept grant, the NSERC Strategic Network for Bioplasmonic Systems (Biopsys) grant, and Biomark Technologies.

#224379 - $15.00 USD Received 7 Oct 2014; revised 27 Oct 2014; accepted 27 Oct 2014; published 3 Nov 2014